Bulletin of Glacier Research 7 (1989) 83－87

Radiation balance in the Gozha Glacier region, in the West Kunlun Mountains

XIE Yingqin[1], KANG Xingcheng[1] and Shuhei TAKAHASHI[2]

1 Lanzhou Institute of Glaciology and Geocryology, Academia Sinica, Lanzhou, China

2 Kitami Institute of Technology, Kitami, 090 Japan

(Received December 9, 1988; Revised manuscript received January 23, 1989)

Abstract

The radiation components (direct solar radiation, diffuse radiation, reflected radiation and effective long-wave radiation) were observed on soil and firn surfaces around the Chongce Ice Cap in the West Kunlun Mountains in summer 1987. The observed maximum daily global radiation was 34.1 MJ/m²d. The reflected radiation was 70% of global radiation on the firn surface, whereas it was lass than 20% on the soil surface. The effective radiation (outgo) is small on the firn surface, less than 20% of the global radiation, while it was about twice that on the soil surface. Consequently, the radiation balance was 2.6－4.4 MJ/m²d on the firn surface (less than 20% of global radiation), whereas it was 10.5－18.2 MJ/m²d on the soil surface (40－70% of the global radiation).

1. Introduction

The West Kunlun Mountains are located in the desert climate area between the Taklimakan Desert and Tibet Highland. The snowline in this area is very high (near 6000m a.s.l.) because of the small precipitation. On the glaciers at high altitudes in this area, the heat balance and water balance should be different from other areas, which are important to examine the mechanism of glacier formation and water circulation. As a part of heat balance observation, the radiation balance was observed during the Sino-Japanese Joint Glaciological Expedition in 1987. The radiation components were observed at three places: near the snowline of the Chongce Ice Cap, at Base Camp and on the bank of Gozha Lake. The method and results of the observation are reported in this paper.

2. Observation points, methods and instruments

2.1. Location of the observation points and conditions of the underlying surface

(1) Point GH-1:

Situated at the juncture of the snowline and the main stream of Chongce Ice Cap (35°14'N, 81°03'E, 6000m a.s.l.) with firn surface, slope direction S25°E, slope 4.6° with almost no shadowing effect of the surrounding mountains to the east, south or west. The biggest shadowing angle in the northern direction is only 5.4°. Two periods of day and night observation were done during August 5－7 and August 15－18.

(2) Point GH-2:

Situated at the Base Camp on the east bank, 1200m downstream from the juncture of the Gozha River and Tianshui River (35°09'N, 81°03'E, 5260m a.s.l.), with sandy soil as its underlying surface, sparsely dotted with grass. The shadowing angle of surrounding mountains was below 6.0°. Day and night observations were done during July 15－20.

(3) Point GH-3:

Situated on the north beach of Gozha Lake nearly 100m from the lake (35°04'N, 81°06'E, 5100m a.s.l.), the surface condition and vegetation were the same as at GH-2. The biggest shadowing angle was not more than 4.0°. Day and night observation was done during August 25－28.

2.2. Methods and instruments

Local mean solar time was used in the time re-

cording. The following three time series were used in each of the observations: 0, 3, 6, 9, 12, 15, 18, 21, 24; 1, 7, 10, 13, 16, 19; 0, 2, 4, 6, 8, 10, 12, 14, 16, 18, 20, 22, 24. The observed items are global solar radiation, direct solar radiation, reflected radiation, radiation balance, cloud cover, cloud form, air temperature, humidity and wind speed gradient (0.5m, 1.0m and 2.0m above the surface), snow/soil temperature (0, 5, 10, 15, 20cm deep), soil moisture and unit weight. The radiation observations were made by DFY-4 type global radiometer, DFY-3 type automatic tracking direct radiometer, CN-2 type radiation balance meter, and aspirated psychrometer. These instruments, except for the CN-2 type radiation balance meter, were all made in China.

3. Components of radiation balance

The difference of radiation energy received and delivered by the underlying surface is defined as radiation balance, denoted by B:

$$B=G(1-R_e)-B_{eff}, \quad (1)$$

where G is the global radiation (W/m²), R_e is the albedo, and B_{eff} is the effective radiation (W/m²) (net long-wave radiation).

The following analysis is based on data observed during the expedition.

3.1. Direct solar radiation

The intensity of direct solar radiation S was observed by instrument and its vertical component S' was calculated with the following formula:

$$S'=S \sin(h) \quad (2)$$

where h is elevation angle of the sun. The direct solar radiation depends on the absorption by water vapor and other gases, the Rayleigh scattering by atmosphere and the Mie scattering by dust. The absorption and scattering relate to an optical path length through the atmosphere. At high altitude of this area (above 5000m a.s.l.), the direct solar radiation is expected to be large because of the small optical path length due to the small atmospheric pressure (below 500mb). The maximum direct solar radiation observed at site GH-2 on July 19 was 1.039×10^3W/m² and its vertical component was 9.49×10^2W/m², from which a transparency is obtained as 0.79. This transparency is relatively large in comparison with that of other stations at sea-level, but not so large as expected for this altitude. It may be affected by dust from Taklimakan Desert or by the relatively high water vapor pressure in the observation period.

Fig. 1 shows the diurnal variations of vertical component of the direct solar radiation in fine days at different altitudes. The variation is very small from 8h to 16h, and changes abruptly before 8h and after 16h; the curve is symmetrical with 12h as its center point. Radiation intensity increases with increase in altitude.

3.2. Diffuse radiation of the sky and global radiation

The diffuse radiation of the sky (D) is another component of global radiation. It depends upon weather conditions, usually being greater on cloudy days than in fine days. The maximum D was 9.3×10^2W/m² on snowy days, 4.3×10^2W/m² on cloudy days and $3.7\times$

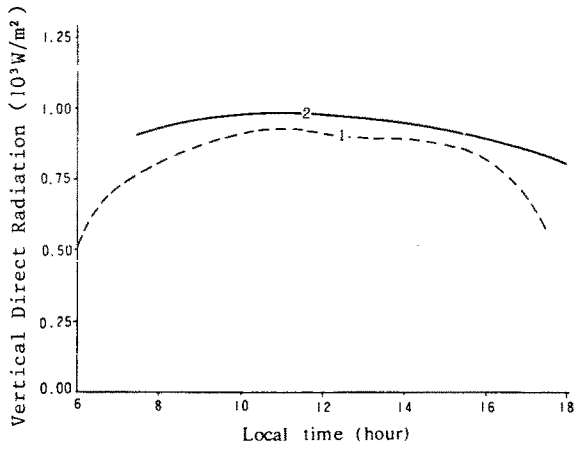

Fig. 1. Diurnal variation of vertical direct radiation at different heights (1: at 5100m a.s.l. and 2: at 6000m).

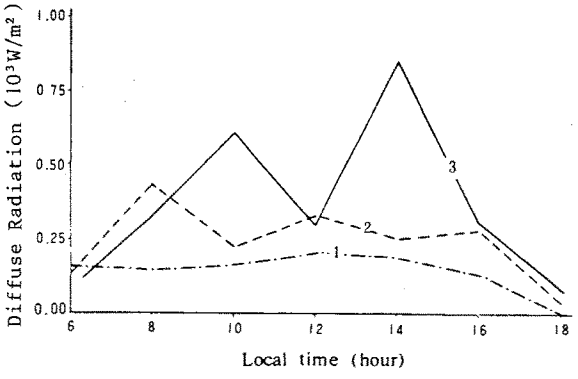

Fig. 2. Diurnal variation of diffuse radiation at different weather conditions at 6000m a.s.l. (1: on fine days, 2: on cloudy days, and 3: on snowy days).

$10^2 W/m^2$ on fine days. On the curve of diurnal variation, the peak value appears around noon on fine days, and there appear several peaks on cloudy or snowy days. The times of occurrence of peaks depend on the cloud cover, cloud form and cloud height. The amplitude of daily variation is large on snowy days (in Fig. 2).

The global radiation is a combination of diffuse radiation and direct solar radiation, therefore, the diurnal variations of the global radiation and its two components are very similar; all the peaks appear around noon, the two sides being symmetrical with the peak as the center (Fig. 3).

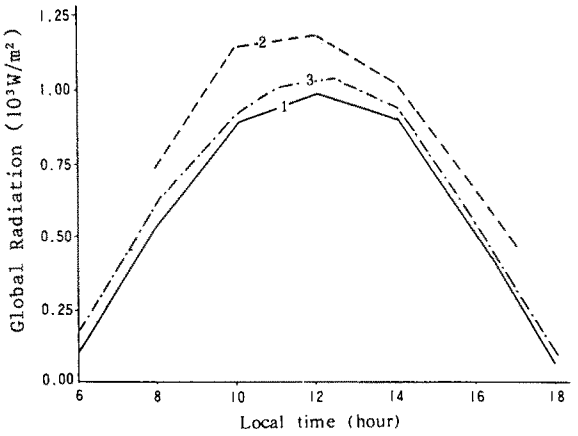

Fig. 3. Diurnal variation of global radiation on fine days at different heights (1: at 5100m, 2: at 5260m, and 3: at 6000m).

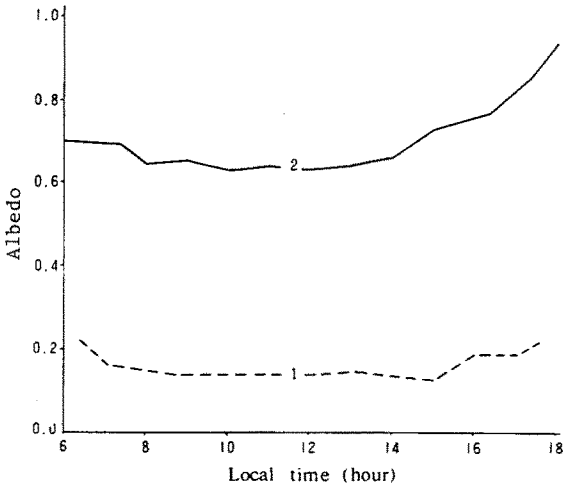

Fig. 4. Diurnal variation of albedo on different underlying surfaces (1: on a soil surface and 2: on a snow surface).

3.3. Reflected radiation on the underlying surface

The reflected radiation (R_k) depends on the conditions of the underlying surface, the weather condition, and the elevation angle of the sun. Fig. 4 shows the diurnal variations of the albedo of snow and soil surfaces on fine days. The albedo around noon was about 0.65 on a snow surface and about 0.15 on a soil surface. The albedo on both surfaces increases with decrease of elevation angle of the sun in the morning and evening. The high albedo in the evening on a snow surface can be attributed to the inclined surface (direc-

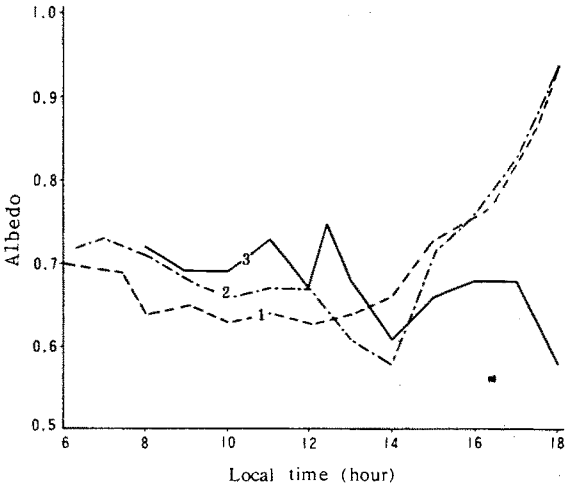

Fig. 5. Diurnal variation of albedo on a snow surface under different weather conditions (1: on fine days, 2: on cloudy days, and 3: on snowy days).

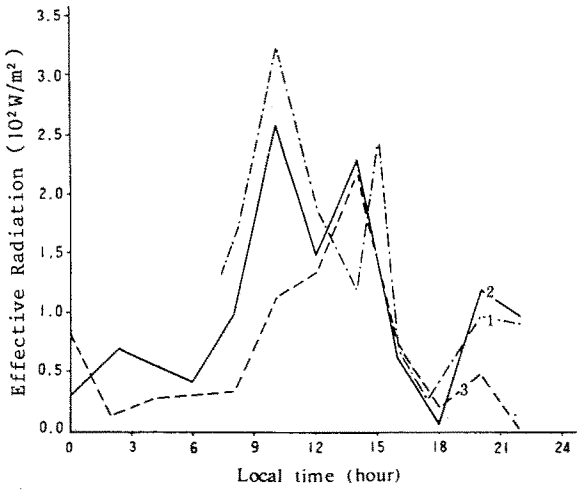

Fig. 6. Diurnal variation of effective radiation under different weather conditions (1: on fine days, 2: on cloudy days, and 3: on snowy days).

tion S25°E, slope 4.6°).

Fig. 5 shows the diurnal variations of albedo on a snow surface in different weather conditions. The forms of the curves in cloudy days and fine days are nearly the same, but the high value in the evening cannot be seen in the snowy day. This difference can be explained by the lack of direct solar radiation on the snowy day, however the albedo at 18h has not so much accuracy.

3.4. *Effective Radiation*

Effective Radiation (B_{eff}) is the difference between long-wave radiation from the underlying surface and atmospheric counter radiation (outgo is defined positive). It was obtained by a radiation balance meter at night, but in daytime by the radiation balance equation indirectly.

The effective radiation mainly depends on air temperature, vapor content in the air, surface temperature, and emissivity of the surface. The daily total effective radiation on soil surface was much larger than that on a snow surface (12.7 MJ/m²d on a soil surface, 5.4 MJ/m²d on a snow surface), which is easy to understand that the temperature on a soil surface is usually higher than on a snow surface.

Diurnal variation of effective radiation on snow surface in various weather conditions is shown in Fig. 6. The effective radiation is large in daytime and small in nighttime, and larger on fine days than on cloudy and snowy days.

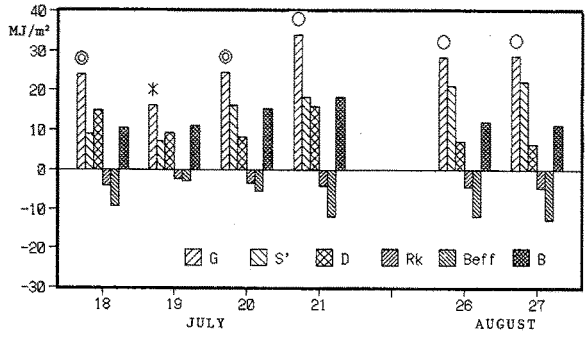

Fig. 7. Radiation components on sandy soil surfaces at GH-2 (July 18–21) and at GH-3 (August 26–27). Circles mean fine day, double circles mean cloudy or overcast day, and an asterisk means snowy day. Notation of radiation components is the same as Table 1.

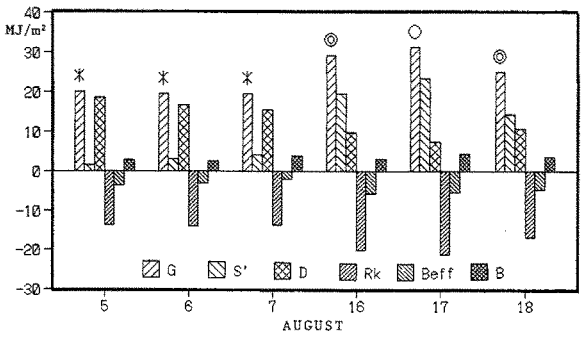

Fig. 8. Radiation components on firn surface at GH-1 (August 5–7 and 16–18). Notation is the same as in Fig. 7.

Table 1. Daily total radiation balance and its components in the Gozha Lake area in the West Kunlun Mountains. G: global radiation, S': vertical component of direct solar radiation, D: diffusu radiation, R_k: reflected radiation, B_{eff} effective radiation (outgo), and B: radiation balance (income). Values in parentheses are percentages of the global radiation G.

Station (Surface)	Location (Altitude)	Date Weather	G MJ/m²d	S' MJ/m²d	D MJ/m²d	R_k MJ/m²d	B_{eff} MJ/m²d	B MJ/m²d
GH-2	35°09'N	July 18 Cloudy	24.1	9.1 (38)	15.0 (62)	4.1 (17)	9.4 (39)	10.6 (44)
(Soil)	81°03'E	July 19 Snowy	16.3	7.1 (44)	9.2 (56)	2.3 (14)	2.9 (18)	11.1 (68)
	(5260m)	July 20 Cloudy	24.4	16.1 (66)	8.3 (34)	3.4 (14)	5.4 (22)	15.5 (64)
		July 21 Fine	34.1	18.3 (54)	15.9 (47)	4.1 (12)	11.9 (35)	18.2 (53)
GH-1	35°14'N	Aug. 5 Snowy	20.0	1.4 (7)	18.6 (93)	13.8 (69)	3.5 (18)	2.7 (14)
(Firn)	81°08'E	Aug. 6 Snowy	19.7	2.9 (15)	16.8 (85)	13.9 (70)	3.2 (16)	2.6 (13)
	(6000m)	Aug. 7 Snowy	19.5	4.0 (21)	15.5 (79)	13.7 (70)	2.1 (11)	3.7 (19)
		Aug. 16 Cloudy	29.2	19.5 (67)	9.7 (33)	20.2 (69)	5.8 (20)	3.2 (11)
		Aug. 17 Fine	31.1	23.6 (76)	7.6 (24)	21.3 (68)	5.4 (17)	4.4 (14)
		Aug. 18 Overcast	25.1	14.3 (57)	10.8 (43)	16.8 (67)	4.7 (19)	3.6 (14)
GH-3	35°04'N	Aug. 26 Fine	28.5	21.2 (74)	7.3 (26)	4.5 (16)	11.9 (42)	12.0 (42)
(Soil)	81°06'E	Aug. 27 Fine	28.5	22.1 (78)	6.4 (22)	4.6 (16)	12.7 (45)	11.3 (39)
	(5100m)							

4. Radiation balance

The radiation balance is depends on both the weather conditions and the underlying surface. The weather affects global radiation and long-wave atmospheric radiation , and the surface affects reflected radiation and long-wave radiation from the surface. The most effective factors controlling the radiation balance are global radiation and albedo, which are also physical factors influencing glacier development, such as advance and retreat, accumulation and ablation.

The combination of radiation balance and its components is very intricate, as shown in Table 1. From these data, the data on soil surface (at GH-2 and GH-3) are graphed in Fig. 7, and the data on firn surface (at GH-1) are in Fig. 8. The characteristics of the components are described below.

(1) Global radiation (G) is related to weather conditions. The maximum daily amount of radiation (34.1 MJ/m²d) appears on fine days, the minimum (16.3 MJ/m²d) appears on snowy days.

(2) The reflected radiation (R_k) on a snow surface is about 70% of the global radiation, whereas that on soil surface is no more than 20%. Variations of above percentages caused by weather conditions did not exceed 5%.

(3) The effective radiation (B_{eff}) on a snow surface is no more than 20% of the global radiation (G) because of its low temperature, only half of that on a soil surface. Variation in the above percentages caused by weather conditions can reach 10% on a snow surface and 20% on a soil surface; the effective radiation on fine days may be three times that on snowy days.

(4) The influence of the underlying surface is very strong. On a sandy soil surface sparsely covered with grass (at GH-2 and GH-3), the radiation balance (B) ranges from 10.5 to 18.2 MJ/m²d, occupying 40—70% of the global radiation. On snow/ice surface (at GH-1), the radiation balance (B) varies within 2.6—4.4 MJ/m²d, occupying less than 20% of the global radiation. The influence of weather conditions on (B) is relatively small, whereas the global radiation is affected by weather conditions largely.

Acknowledgment

The authors would like to express their thanks to Associate Professor Bai Chong Yuan for his precious advice.